



Effect of Nitrate Concentration on Anaerobic Methane Oxidation Coupled to Denitrification in Membrane Biofilm Reactor After Prolonged Storage

Wei Zhang · Yibo Zhao · Jing Wang · Yang Gao ·
Lean Zhou · Shiquan Sun · Meiyi Tang ·
Yazhou Peng · Wenbing Guo · Hongyu Wang

Received: 5 November 2023 / Accepted: 13 March 2024 / Published online: 8 April 2024
© The Author(s), under exclusive licence to Springer Nature Switzerland AG 2024

Abstract The effects of the influent nitrate (NO_3^- -N) concentration on reactor performance and microbial communities of anaerobic methane oxidation coupled to denitrification in a membrane biofilm reactor were emphatically investigated after prolonged storage. The system was run for a period of 185 days including the storage period, reactivating process, and stable operation phase. The influent NO_3^- -N concentrations varied from 10, 20, and 30 mg/L, and the reactor was continuously operated for 135 days. The denitrification rate in the reactor was

activated first and then inhibited, with the average value of NO_3^- -N consumed of $0.42 \text{ mg/L}\cdot\text{h}^{-1}$ at influent NO_3^- -N of 20 mg/L; there was no obvious nitrite and ammonia-nitrogen accumulation in the whole stage. Illumina MiSeq sequencing results showed that increases in NO_3^- -N loading could improve the microbial abundance in the system. The highest value for variety and the lowest value for the evenness of the microbial community corresponded to the ideal value of 20 mg/L. It speculated that promoting biofilm bacteria (PBB) became the key functional bacterial group after prolonged storage. Besides, the abundance of methane-oxidizing bacteria was significantly increased in synergy with PBB and denitrifiers to achieve reactivating and stable operation of anaerobic methane oxidation coupled to denitrification.

W. Zhang · Y. Zhao · Y. Gao · L. Zhou · S. Sun
School of Hydraulic and Environmental Engineering,
Changsha University of Science & Technology/Key
Laboratory of Dongting Lake Aquatic Eco-Environmental
Control and Restoration of Hunan Province,
Changsha 410114, China

J. Wang
Central and Southern China Municipal Engineer Design &
Research Institute Co. Ltd, Wuhan 430072, China

M. Tang
China West Construction Hunan Group Co. Ltd.,
Changsha 410114, China

Y. Peng
College of Civil Engineering, Hunan University of Science
and Technology, Xiangtan 411201, China

W. Guo · H. Wang (✉)
School of Civil Engineering, Wuhan University,
Wuhan 430072, China
e-mail: hywang96@126.com

Keywords Electron donor · Anaerobic methane oxidation · Continuous flow reactor · Nitrogen removal · Heterotrophic/autotrophic denitrification · Microbial diversity

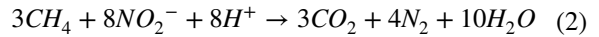
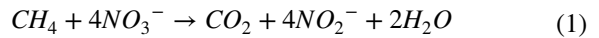
1 Introduction

Nitrate (NO_3^- -N) is considered to be one of the most common pollutants in the world (Elmelouky et al., 2018). Studies have shown that significant amounts of NO_3^- -N, which are typically released into water from industrial, agricultural, and domestic wastewater, not only cause eutrophication and water quality damage,

but also have harmful effects on human health, especially for children including methemoglobinemia (Massoudinejad et al., 2018; Romanelli et al., 2020). To remove excess NO_3^- -N, common treatment methods can be divided into biological denitrification, chemical and physicochemical methods (Zolnierczyk & Barbusinski, 2019). Biological denitrification with its high efficiency, low cost, and stable operation has been widely applied (Liu et al., 2019). However, low carbon-to-nitrogen ratio is the characteristics of real domestic wastewater in China, leading to the lack of electron donors for denitrification.

To date, selection and optimization of suitable electron donors is a hot topic in this field (Ding et al., 2017a; Pu et al., 2014). Like that, autotrophic denitrification uses inorganic carbon sources (such as CO_3^{2-} and HCO_3^-) as electron donors such as hydrogen gas (Luesken et al., 2011), sulfide (Ghafari et al., 2008), and iron compounds (Zhou et al., 2016) were chosen as electron donors for denitrification. Recently, it has been reported that methane (CH_4) can be indirectly used as an electron donor for denitrification under anaerobic conditions. This process has been found in both natural environment and engineering systems (Luesken et al., 2011; Smith et al., 1991), like the so-called denitrification-dependent anaerobic methane oxidation (DAMO) technology (Ding et al., 2017b). For instance, Lou et al. have investigated the effects of temperature, pH, and dissolved oxygen on the DAMO process (Lou et al., 2020); denitrification can be achieved by co-enrichment of DAMO microorganisms and anaerobic ammonia oxidizing bacteria in a biofilm reactor (Shi et al., 2013). The following Eqs. (1) and (2) show the reaction process of the DAMO process using NO_3^- -N (or NO_2^- -N) as the oxidant (Harb et al., 2021a). On the one hand, it cannot only significantly reduce the emission of the CH_4 in the sewage treatment process, but also greatly reduces the operating cost of the denitrification treatment process due to the addition of an organic carbon sources (Cao et al., 2021). Besides, previous literature pointed that simple organics (e.g., short chain fatty acids) could be produced during anaerobic CH_4 oxidation process, implying that heterotrophs or/and autotrophs being fed with these intermediates simultaneously (Guo et al., 2023). However, the CH_4 -driven denitrification system is very strict with the system environment and the functional microbes grow slowly, resulting in the difficult enrichment of microorganisms and its practical application

(Bhattacharjee et al., 2016; Lim et al., 2021), while the studies of enrichment of these functional microorganisms with stable operation in bioreactor configurations are still insufficient. Besides, the works focused on the functions and relationships among the functional bacteria are still limited.



Inspired by monitoring the growth of functional bacteria by nitrification intensification process to significantly reduce microbial metabolites and improve reactor efficiency (Sepehri & Sarrafzadeh, 2019). Nitrogen feeds (such as N concentration and source type) is important for the microbial composition in the anaerobic methane oxidation coupled to denitrification co-culture system (Harb et al., 2021b). Besides environmental factors, the co-culture system may also encounter system storage and idleness problems, but not many studies have been conducted in this area. And cold storage is a common means for microbial system preservation. For example, Shen et al. studied the frozen storage and reactivation of microalgal-bacterial granular sludge (Shen et al., 2021). There are not many studies on reactivation following reasonably lengthy storage in biological reactors, much alone the reactions to the microbial populations, as far as we know. The reactor was firstly stored at below 12 °C for 25 days, and then recovered in a continuous reactor within 25 days. Thus, the purpose of this work was to examine the restart-up, long-term operation of denitrification and anaerobic methane oxidation coupled to membrane biofilm reactors, as well as the reactor performance with different influent NO_3^- -N concentrations and corresponding changes in the microbial community following the recovery period. The results will help to provide a useful theoretical basis for the application of the CH_4 -driven denitrification technology in practical sewage treatment for reactivation in response to fluctuating nitrate concentration loads.

2 Materials and methods

2.1 Inoculation sludge and simulated wastewater

The inoculation sludge in the experiment was taken from the secondary sedimentation tank in Wuhan

Shahu Sewage Treatment Plant, and the initial MLSS of the precultured sludge was about 8900 mg/L. It was placed in a 5-L closed container for a month of domestication, and then the sludge culture liquid (20 mg/L NO_3^- -N, 25 mg/L K_2HPO_4 , 20 mg/L KH_2PO_4 , 10 mg/L CaCl_2 , 2000 mg/L NaHCO_3 , and 0.5 ml/L trace element solution) was added to the container to multiply the microorganisms, replaced the fresh sludge culture liquid every day, and introduced 15 min nitrogen to form an anaerobic environment. Sufficient CH_4 gas was then introduced to achieve the purpose of cultivation and domestication.

The influent used in the reactor was synthetic wastewater which consisted of 10–30 mg/L NO_3^- -N, 25 mg/L K_2HPO_4 , 20 mg/L KH_2PO_4 , 10 mg/L CaCl_2 , 2000 mg/L NaHCO_3 , and 0.5 mL/L trace element solution. Trace element solution was composed of 0.5 g/L $\text{ZnSO}_4 \cdot 7\text{H}_2\text{O}$, 2 g/L CaCl_2 , 2.5 g/L $\text{MnCl}_2 \cdot 4\text{H}_2\text{O}$, 10 g/L $\text{Na}_2\text{MoO}_4 \cdot 4\text{H}_2\text{O}$, 0.18 g/L KI, 0.18 g/L $\text{CuSO}_4 \cdot 5\text{H}_2\text{O}$, 0.18 g/L $\text{CoCl}_2 \cdot 6\text{H}_2\text{O}$, and 0.18 g/L $\text{FeCl}_3 \cdot 6\text{H}_2\text{O}$. All the chemicals used in the present study were of analytical grade.

2.2 Experimental equipment and operation

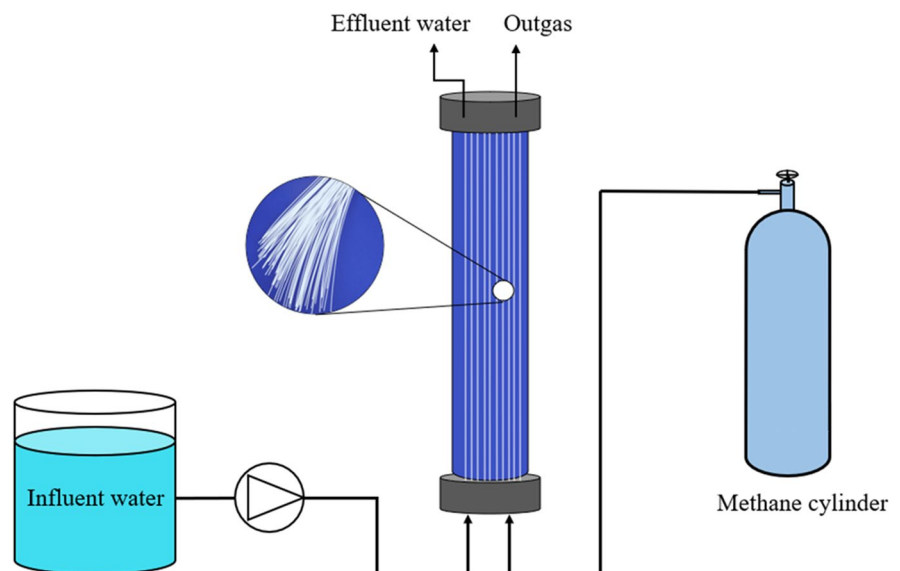
The continuous flow reaction device used in this test was shown in Fig. 1. The external reaction tank was made of plexiglass and had a cylindrical shape. The internal hollow fiber membrane was made of polyvinylidene difluoride material, which had good heat

resistance and chemical stability, and the pore shape was round and oval, and the pore diameter is between 0.2 and 0.3 μm . The reactor unit height was 300 mm, the inner diameter was 100 mm, and the total effective volume was 1.25 L.

The entire reactor was protected from light to reduce the effect of lighting. The reactor continuously pumped water from the catchment vessel and flowed out from the water outlet in the middle of the upper end of the reactor from bottom to top. CH_4 came out of the cylinder and was directly connected to the intake port at the lower end; the influent pressure was 0.01 MPa (~50 min/day). The unreacted and reacted gas is discharged from the upper exhaust port and collected for treatment. After MBfR with arrange mud law, the reactor has already continued to operate stably for 190 days, with stable NO_3^- -N removal of approximately 50%.

The reactor was exposed in below 12 °C for 25 days (storage period) and recovered under the condition of continuous flow within 25 days (reactivating process, data not shown here). After this, the stable operating phase was divided into three phases based on the pertinent conditions, with the influent NO_3^- -N concentration was 10 mg/L (day 1–25), 20 mg/L (day 56–80), and 30 mg/L (day 111–135), respectively. Extra adjustment period about 30 days was carried out when each stage ends. During the extra adjustment period, the nitrate load for the next stage was run on a trial basis to ensure stable reactor operation;

Fig. 1 Scheme of the reactor



other operating conditions of the reactor were pH=7.5, HRT=20 h, and the temperature = ~20 °C. Finally, the effects of different influent water NO_3^- -N concentrations on the microbial population structure in the system were further investigated.

2.3 Analytical methods and Illumina MiSeq sequencing

NO_3^- -N was measured according to the ultraviolet spectrophotometry method, while that of nitrite (NO_2^- -N) was using N-(1-naphthyl)-ethylenediamine spectrophotometry method, ammonia–nitrogen (NH_4^+ -N) was Nessler reagent spectrophotometry method (Xu et al., 2022b). TIN represented the sum of all the above three values. pH was measured using a pH meter (METTLER TOLEDO). Sludge samples under different working conditions were collected for high-throughput sequencing, and the changes in microbial population structure were analyzed at the microscopic level. All sequencing in this trial was performed at Majorbio (Shanghai, China), using the Illumina Miseq platform, with 515F (5'-GTGCCA GCMGCCGCGGG-3') and 907R (5'-CCGTCA ATTCTTTTRAGTTT-3') as primers for PCR amplification and pyrosequencing according to previous research (Wang et al., 2018). The sequencing results were marked as S1, S2, and S3 corresponding to the 25th, 80th, and 135th day at stable operation phase, respectively.

3 Results and discussion

3.1 The effects of the influent NO_3^- -N concentration on denitrification process

The experiment in this stage mainly explored the removal of NO_3^- -N by the reactor when the influent NO_3^- -N concentration was 10 mg/L, 20 mg/L, and 30 mg/L, respectively. Excluding reactivation, the reactor had been further continuously operated for about 135 days. During the stable operation of the reactor, the concentration of NO_3^- -N in the influent and effluent, the removal rate of NO_3^- -N, and the accumulation amount of NO_2^- -N by different influent NO_3^- -N concentrations were shown in Fig. 2.

As shown in Fig. 2a–d, the influent NO_3^- -N concentration had a great impact on the denitrification performance of the reactor, which was manifested in the fact that the removal efficiency of NO_3^- -N in the reactor gradually decreased with the increase of the influent NO_3^- -N concentration (Vasiliadou et al., 2009). Accordingly, for NO_2^- -N, the effluent concentration and accumulation of NO_2^- -N increase in value with increasing of NO_3^- -N loading from 10 to 30 mg/L; for NH_4^+ -N, the effluent concentration and accumulation of NH_4^+ -N under different NO_3^- -N loading showed a gradually decline; for TIN, the removal efficiency and accumulation of TIN was gradually decreased with a trend of variety of NO_3^- -N keeping consistently.

Fig. 2 Variation of NO_3^- -N, NO_2^- -N, NH_4^+ -N, and TIN in the continuous experiments for different influent nitrate concentrations (stage I: 0–25 days, stage II: 56–80 days, and stage III: 111–135 days)

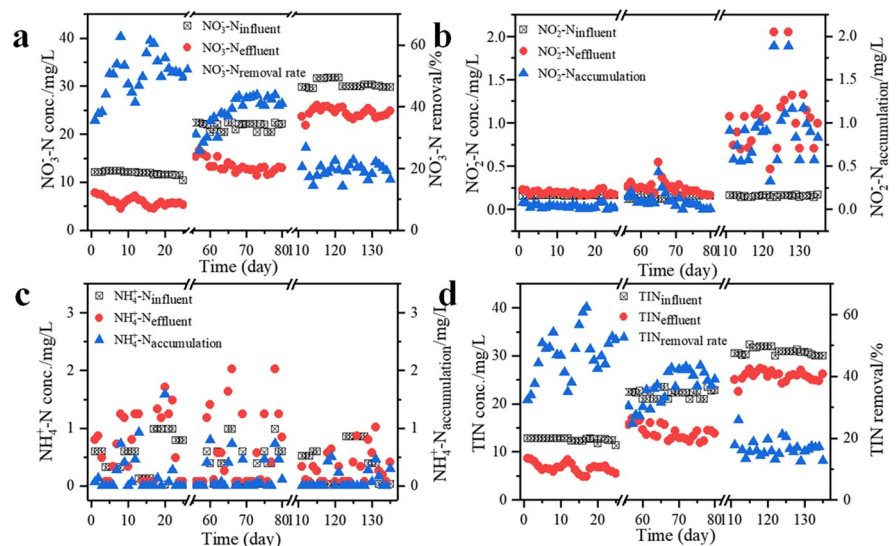


Figure 3a, b shows the average removal performance of NO_3^- -N with different NO_3^- -N loading. At influent NO_3^- -N concentration of 10, 20, and 30 mg/L, the average removal efficiency of NO_3^- -N was approximately 50.0%, 38.4%, and 19.5%, respectively, while the denitrification rate of the system was firstly increased and then decreased, with the optimum of denitrification rate of NO_3^- -N of 0.42 mg/L·h⁻¹ at NO_3^- -N of 20 mg/L. It suggested that the biological system had a certain tolerance to the impact of influent NO_3^- -N concentration. At a certain influent NO_3^- -N loading, it might provide a favorable condition for the growth and reproduction of microbes, which ultimately enhance the ability of denitrification process; furtherly, the enzymatic reaction rate might also be accelerated within a certain range of concentration of the substrate. But previous literature also pointed that nitrate reductase could be inhibited by higher concentration of NO_3^- -N (Deigl-mayr et al., 2006). In addition, the removal efficiencies of nitrate were only ~50% probably due to the low pressure of the influent CH_4 (0.01 MPa, 50 min/day), which might result in insufficient supply quantity of CH_4 , thus resulting in a low nitrate removal rate. Specifically, the mass transfer of CH_4 is critical for the enrichment of microorganisms in the reactor,

but CH_4 is a very poorly water-soluble gas, and insufficient CH_4 in the dissolved state will result in the normal growth of microorganisms not being guaranteed. In Cai's research, by changing the inlet mode of the reactor methane supply, they found that when the CH_4 volume concentration was 20%, the denitrification rate was 2.76~2.81 mg/L·h⁻¹ and when the CH_4 volume concentration increased to 100%, the denitrification rate was 9.3 mg/L·h⁻¹ (Cai, 2013).

As shown in Fig. 3c–e, it was worth noting that the accumulation of NO_2^- -N was very low at stage I and II. As the influent NO_3^- -N concentration increased to 30 mg/L, the average accumulation amount of NO_2^- -N increased rapidly compared with stage I and II, with value of approximately 0.89 mg/L. The incomplete reaction of denitrification process might be responsible for the cumulative increased in NO_2^- -N with the influent NO_3^- -N concentration of 30 mg/L, which was also similar to the previous reported work (Chen et al., 2016). Additionally, there was no significant accumulation of NH_4^+ -N at three stages, with a relatively steady level of 0.2 mg/L. The TIN removal observed was close to change trend of NO_3^- -N removal, but the former is little lower than the latter, resulting from synergistic effect of functional microorganism. Comparison with other

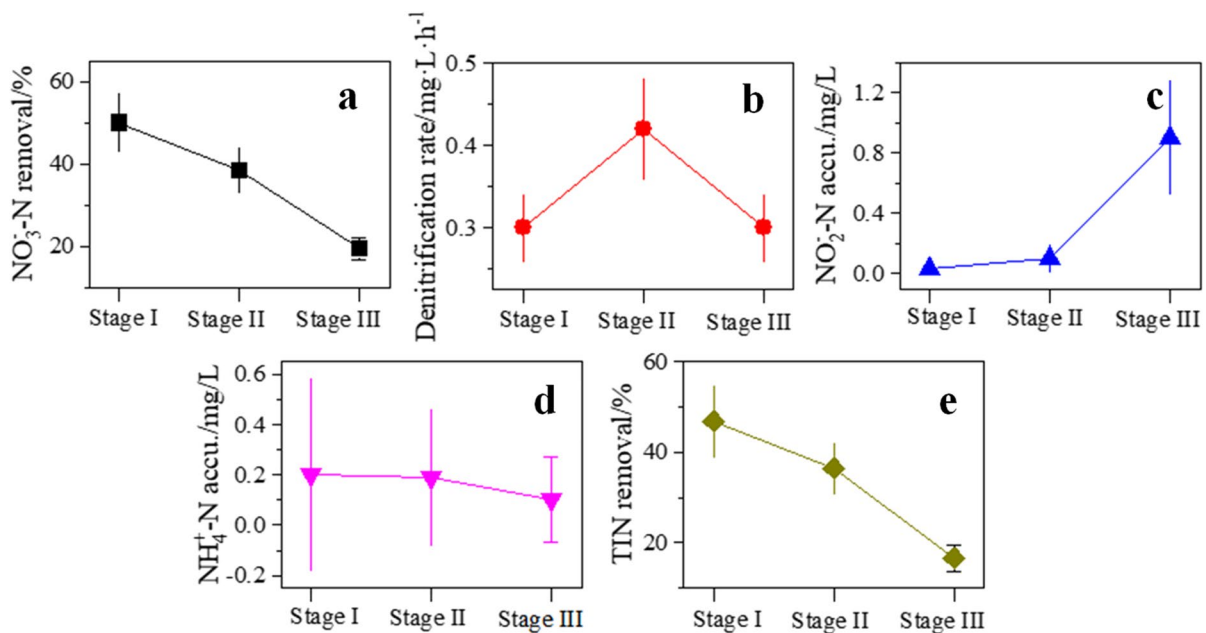


Fig. 3 The average effluent characteristics of NO_3^- -N, NO_2^- -N, NH_4^+ -N, and TIN under different stages

electron donors such as hydrogen (Puig et al., 2012), $\text{FeSO}_4 \cdot 7\text{H}_2\text{O}$ (Wang et al., 2017), and sulfur (Wang et al., 2016) let alone of organics for denitrification, the value of denitrification rate achieved in this work was not high, whereas good benefit in economy and environment may be achieved.

3.2 Richness and diversity of microbial communities

Sludge was selected for high-throughput sequencing at each stage when the system was in stable operation, and the sequencing results are marked as S1 (stage I), S2 (stage II), and S3 (stage III). Based on the alpha diversity analysis of the three samples, the comprehensive analysis results of the abundance and diversity of the microbial populations in the reactor were shown in Table 1.

As can be seen from Table 1 that a total of 38,423, 51,605, and 48,710 effective sequences were generated from three samples, and coverage index of the three samples were all greater than 0.996, indicating that the sequencing result was highly reliable and the effective sequences can cover most area (Wang et al., 2019b). The sequencing depth could well represent the microbial community in the three samples, and the result could reflect the true conditions of the samples effectively. Ace and Chao indices showed the same changing trend, increasing with the increase of the influent NO_3^- -N concentration; the order was $\text{S3} > \text{S2} > \text{S1}$. It indicated that an appropriate increase in the concentration of NO_3^- -N could increase the species abundance in the reactor, which might be caused by the increase of the nitrogen source for the growth of microbial, also promoted the species reproduction. Shannon and Simpson indices could represent the biodiversity of the sequencing samples. The larger the Shannon, the smaller the Simpson, indicating that the diversity of microbial was higher (Khanina et al., 2016). Therefore, the three samples were sorted as $\text{S2} > \text{S3} > \text{S1}$ by diversity. It indicated that an appropriate increase

of the influent NO_3^- -N concentration was conducive to the coexistence of multiple microbial in the reactor. Shannoneven and Simpstoneven indices reflected the uniformity of samples. The larger Shannoneven and the smaller Simpstoneven, the better the uniformity of microbial (Wang et al., 2019a). The three samples were sorted as $\text{S2} > \text{S3} > \text{S1}$ by uniformity. When the influent NO_3^- -N concentration was 10 mg/L, the microbial diversity and uniformity in the reactor were the smallest. It might be caused by the relatively low nitrogen source environment at the beginning, which was not conducive to the growth and reproduction of microbes, and had a certain selective effect on the types of microbial.

The above result was the same as the result shown in the dilution curve and the grade-abundance curve in Fig. 4a, b. The dilution curves of the three samples tended to be flat eventually, indicating that the sampling of this sequencing was rational. The continuing increase of the reads number could only produce a small amount of OTUs. The grade-abundance curve showed that when the influent NO_3^- -N concentration was 10 mg/L, the horizontal width was the narrowest and the curve was the steepest, which indicated that the abundance of microbial in the reactor was the lowest and the uniformity was the worst at this level. Non-repetitive sequences were clustered by OTUs on the basis of the 97% similarity, and the three samples were analyzed by OTUs.

The Venn diagram in Fig. 4c counted the number of common and unique OTUs in the three samples, which intuitively showed the similarity and overlap of the OTUs composition of the samples under different influent NO_3^- -N concentrations. It can be seen from the figure that the total number of OTUs obtained by the three samples was 931, and the numbers of OTUs by S1, S2, and S3 individually were 38, 82, and 104, respectively, accounting for 4.08%, 8.81%, and 11.17% of the total number of OTUs. The number of OTUs shared by the three samples was 483, accounting for 51.88% of the total number of OTUs. The

Table 1 Microbial alpha diversity indices under different NO_3^- -N concentrations

Samples	Reads	OTUs	Ace	Chao	Shannon	Simpson	Shannoneven	Simpstoneven	Coverage
S1	38,423	652	777	799	4.17	0.04197	0.6405	0.03789	0.997
S2	51,605	717	819	841	4.40	0.03681	0.6695	0.03405	0.996
S3	48,710	752	906	914	4.24	0.03906	0.6441	0.03650	0.996

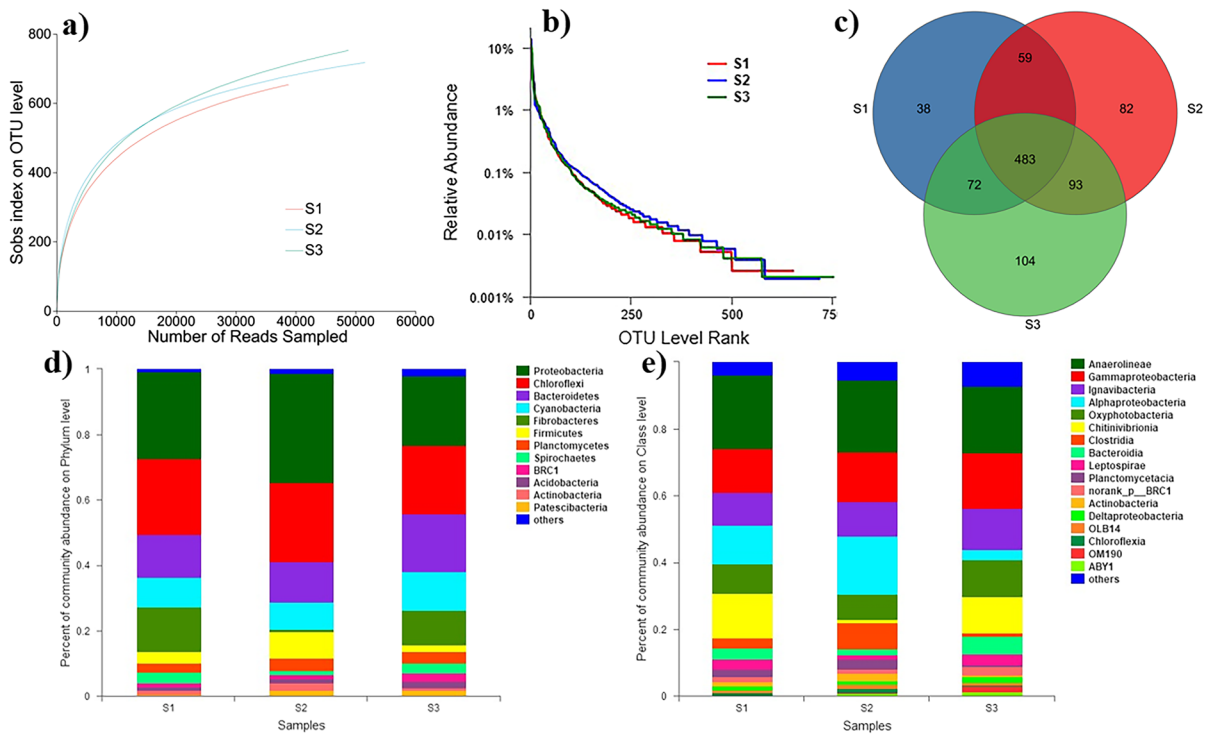


Fig. 4 **a** Dilution curve, **b** rank-abundance curve, **c** Venn diagram, and diagram of relative content of microorganisms at **d** phyla and **e** class levels under different stages

results showed that the microbial populations in the reactor under different influent NO_3^- -N concentrations had higher similarities and less differences. The change in influent concentration did not have a large impact on the microbial community structure in the system; the reactor had a certain denitrification and nitrogen removal capacity in all three stages.

3.3 Structure analysis of microbial community

3.3.1 Phylum-level population distribution

At aqueous NO_3^- -N concentrations of 10 mg/L, 20 mg/L, and 30 mg/L, respectively, microbiological community structure was analyzed for the three samples; a total of 33 phyla were detected. As shown in Fig. 4d, it can be seen that microbial community structure showed great similarity at the phylum level in the three samples, top 6 bacteria of the relative proportion of microbial abundances in the three samples, they were *Proteobacteria*, *Chloroflexi*, *Bacteroidetes*, *Cyanobacteria*, *Fibrobacteres*, and *Firmicutes*. The sum of these bacteria gates accounted for

more than 85% of the three samples, respectively. Among these, *Proteobacteria* represented the highest proportion of the three samples, respectively, at 26.37%, 33.34%, and 21.31%. Secondly, *Chloroflexi* and *Bacteroidetes*, *Chloroflexi* represented 23.41%, 24.23%, and 21.01% of the three samples; *Bacteroidetes* accounted for 13.00%, 12.34%, and 17.62%, respectively. *Proteobacteria* and *Bacteroidetes* had long been regarded as the most common autotrophic denitrification microorganisms during denitrification and nitrogenous species containing various types of denitrification and CH_4 oxidizing bacteria (Luo et al., 2013), which could see the highest relative abundance of *Proteobacteria* at the aqueous NO_3^- -N concentration of 20 mg/L, indicating that the appropriate nitrogen source concentration facilitates microbial proliferation within the reactor, either too high or too low. The change trend of *Chloroflexi* phylum was similar. *Chloroflexi* contained many types of microorganisms, and the anaerobic phylum under this phylum was believed to be able to participate in the process of autotrophic denitrification (Lu et al., 2018; Shu et al., 2015). The relative abundance of *Cyanobacteria*

bacteria in the S1~S3 samples was 9.20%, 8.31%, and 11.84%, respectively. *Cyanobacteria* were likely to produce methane in anoxic environment (Fazi et al., 2021). As shown, the relative abundance of *Fibrobacteres* in S2 was greatly reduced, while that of *Firmicutes* was opposite. The unifying features of *Fibrobacteres* were cellulose hydrolysis, anaerobic metabolism, and lack of motility (Rahman et al., 2016). Additionally, *Acidobacteria*, *Actinobacteria*, *Patescibacteria*, etc., could also be detected in samples, but the relative abundance was low (less than 3%). *Firmicutes* and *Acidobacteria* were shown to have denitrification genes with corresponding denitrification ability and be the dominant phyla in the anammox-denitrification biomass (Wei et al., 2017). *Actinobacteria* could generate soluble electron shuttles in denitrification (Pang & Wang, 2020). *Patescibacteria* were frequently found in groundwater and associated with nitrogen cycling in groundwater (Cao et al., 2022).

3.3.2 Class-level population distribution

Subsequently, the composition of the microbial community structure in the sludge samples at different levels was further analyzed from the class level, and the analysis results are shown in Fig. 4e. The three samples detected a total of 69 species of bacteria. The dominant bacteria in the system were *Anaerolineae*, *Gammaproteobacteria*, *Ignavibacteria*, *Alphaproteobacteria*, *Oxyphotobacteria*, and *Chitinivibrionia*. The sum of these bacteria accounted for more than 70% of the total number of samples. *Anaerolineae* was a typical autotrophic denitrifying bacteria (Xiao et al., 2015), and its relative abundance in the three samples was the highest of 21.95%, 21.55%, and 19.91%, respectively. Among them, *Gammaproteobacteria* and *Alphaproteobacteria* belonged to the phylum *Proteobacteria* and had been proven to be able to remove NO_3^- -N in a number of previous studies on autotrophic denitrification (Liao et al., 2014). When the influent NO_3^- -N concentration was 10 mg/L, the proportion of *Gammaproteobacteria* in the sample was 13.31%. When the influent NO_3^- -N concentration increased, the relative abundance of *Gammaproteobacteria* also increased to 14.93% and 16.63%, respectively. As the concentration of influent NO_3^- -N increased, its relative abundance also increased. The relative abundance of

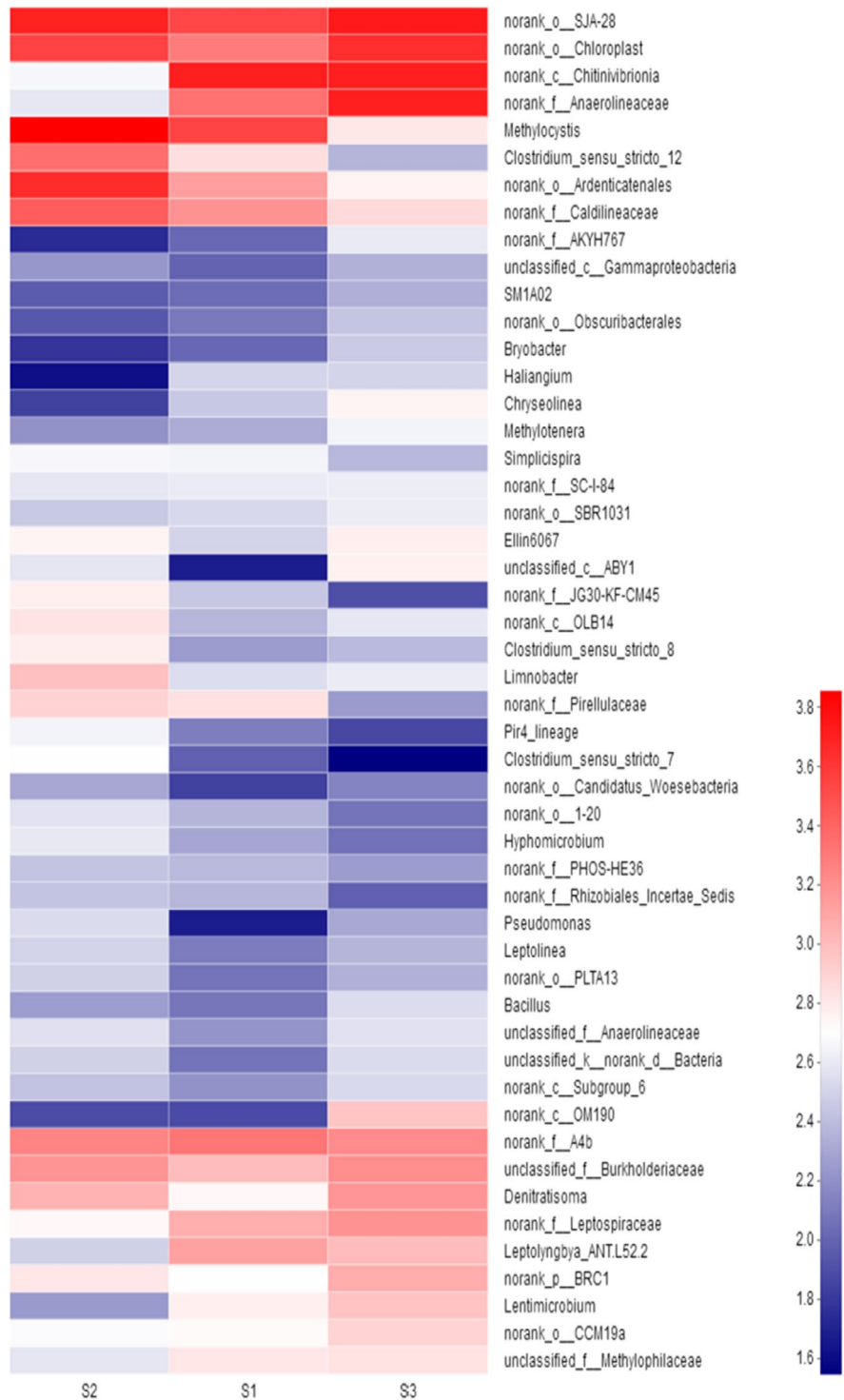
Alphaproteobacteria was the highest among the S2 samples, reaching 17.33%, which indicated that the appropriate nitrogen source concentration was helpful for the proliferation of this type of microorganisms in the reactor. When the concentration was too high or too low, the relative abundance would decline. The change trend of *Oxyphotobacteria* was just the opposite; the relative abundance in S2 was only 7.70%.

3.3.3 Horizontal population distribution of the genus

The 50 bacterial genera with the highest relative abundance of the sample species were selected for the heat map, and the results are shown in Fig. 5. It can be seen that there were certain differences in the distribution of the microorganisms in the three samples at the genus level. Specifically, the 10 genera with the highest relative abundance in S1 and their proportions were *norank_c_Chitinivibrionia* (13.48%), *Methylocystis* (9.21%), *norank_o_SJA-28* (8.89%), *norank_f_Anaerolineaceae* (5.73%), *norank_f_A4b* (5.46%), *norank_o_Chloroplast* (5.13%), *norank_f_Caldilineaceae* (4.05%), *norank_o_Ardenticatenales* (3.65%), *Leptolyngbya_ANT.L52.2* (3.48%), *norank_f_Leptospiraceae* (3.04%), *unclassified_f_Burkholderiaceae* (2.61%), and *norank_f_Pirellulaceae* (1.79%). The 10 genera with the highest relative abundance in S2 and their proportions were *Methylocystis* (13.90%), *norank_o_SJA-28* (9.69%), *norank_o_Ardenticatenales* (8.77%), *norank_o_Chloroplast* (6.84%), *norank_f_Caldilineaceae* (5.32%), *Clostridium_sensu_stricto_12* (4.41%), *norank_f_A4b* (3.50%), *unclassified_f_Burkholderiaceae* (2.96%), *Denitratisoma* (2.14%), and *Limnobacter* (1.88%). The 10 most abundant bacterial genera in S3 and their proportions were *norank_o_SJA-28* (11.27%), *norank_c_Chitinivibrionia* (10.70%), *norank_f_Anaerolineaceae* (10.70%), *norank_o_Chloroplast* (9.13%), *norank_f_A4b* (3.46%), *unclassified_f_Burkholderiaceae* (3.34%), *norank_f_Leptospiraceae* (3.22%), *norank_p_BRC1* (2.43%), *Lentimicrobium* (1.93%), and *norank_c_OM190* (1.89%).

The above data showed that with the change of the influent NO_3^- -N concentration, the dominant bacteria at each level also changed. It can be seen that *Methylocystis*, which could use methane or methane oxidation intermediates as electron donors for denitrification (Lai et al., 2018), had the largest abundance when

Fig. 5 The difference of microbial population dynamics in terms of genus level



the influent NO₃⁻-N concentration was 20 mg/L. With the influent NO₃⁻-N concentration increased or decreased, its abundance would decrease, which

was similar with the results in a previous study (Vasi-liadou et al., 2009). At the same time, the dominant bacteria genus *norank_f__Anaerolineaceae* in the

previous studies (Zhang et al., 2016) on the enrichment of anaerobic methane oxidation and denitrification microorganisms in the hollow fiber membrane bioreactor was also detected, but its abundance was low at 20 mg/L.

3.4 Core functional genera responsible for the denitrification process and mechanisms discussion

As shown in Table 2, there were several main groups of functional bacterial groups including methane-oxidizing bacteria (MOB), heterotrophic denitrifiers (HD), promoting biofilm bacteria (PBB), autotrophic denitrifiers (AD), etc. For PBB, it was clearly observed that the abundance of PBB such as *norank_c__Chitinivibrionia*, *norank_o__SJA-28*, *norank_f__A4b*, and *norank_f__Leptospiraceae* in stage III of the MBfR was higher than that in stage I and II, which benefited to the reconstruction and stability of biofilm via their metabolic process. It is like in a nitrifying-enriched activated sludge system study, nitrifying bacteria produced extremely low extracellular polymeric substance and soluble microbial products, resulting in lower fouling, which similar to the role of PBB (Sepehri & Sarrafzadeh, 2018). Besides, the relatively high nitrate loading could also enrich the PBB. After restarting, a portion of dead microorganisms, even the membrane matrix may be served as carbon source during starvation phase. It was agreed to the rapid increase of abundance of PBB after reoperation. For MOB, neither DAMO archaea nor DAMO bacteria were found in the bacterial community analysis. Unlike typical DAMO bacteria, the dominant bacterial genera capable of oxidizing CH₄ including *Methylocystis*, *Methylotenera*, and *norank_f__methylophilaceae*, were detected in MBfR, which may be responsible for oxidizing CH₄ to methanol or fatty acids for further denitrification (Liang et al., 2022). For example, *Methylocystis* sp. is the common type II methanotroph, uses nitrite as a terminal electron acceptor, and flexibly couples with methane oxidation. This special electron transfer process potentially accelerates methane anoxic oxidation (Liu et al., 2023). *Methylocystis* sp. also was proved to be of important role in bromate and nitrate bioreduction as reported in previous literature (Lai et al.,

2018). The role of these methanotrophs and other methane-oxidizing bacteria (MOB) was most likely to accelerate the denitrification process by converting the produced organics to acetate or hydrogen for denitrifiers or promoting biofilm bacteria. For HD or AD, the extended operation brought irreversible changes to denitrifiers, which could be explained by the competition of electron donors between these bacterial species. HD mainly use organic substrates as electron donors for denitrification, while AD use inorganic substrates for denitrification (Lee et al., 2013). In the extended operation, HD may gradually adapt to and preferentially utilize organic substrates, which are usually more abundant and readily available in MBfR (from the methane oxidation of MOB), leading to relatively faster growth of HD and a relative decrease in the abundance of AD. This competition may further exacerbate irreversible changes in the numbers and functions of both.

The average removal of nitrate nitrogen by the reactor gradually showed a decreasing trend, but the average denitrification rate of the reactor increased and then decreased. The optimum of denitrification rate of NO₃⁻-N was observed when the nitrate load was 20 mg/L. At this time, the microbial community diversity in the system was the greatest and the homogeneity was the smallest, and the relative abundance of MOB was 9.21% and 13.90% in S1 and S2, while it did not enter the top 10 in S3. Based on these, it was speculated that when nitrate load was increased in a certain range, the activity of MOB was enhanced, the methane oxidation rate was accelerated, and the production of readily biodegradable organics increased. Then, these organics were used as electron donors for enrichment or denitrification process of HD and AD, so the denitrification rate was accelerated. However, when the influent nitrate nitrogen load was 30 mg/L, the average nitrite nitrogen accumulation increased, which was inhibitory and toxic for microorganisms, both nitrate nitrogen and denitrification rates decreased. PBB in some certain period also served as converter to degrade refractory substances of membrane base during starvation phase, especially after storing at low temperature and reactivating. Therefore, synergistic system of methanotrophic bacteria, denitrifiers, and PBB was reconstructed in the MBfR (Fig. 6).

Table 2 The key functional groups classification at genus level (top 10 at each stage)

Functional groups	Bacteria	Descriptions	Stage		
			S1 ^a	S2 ^a	S3 ^a
MOB	<i>Methylocystis</i>	Type II methanotroph (Semrau et al., 2011)	9.21%	13.90%	–
PBB	<i>norank_c__Chitinivibrionia</i>	Heterotrophic bacteria showed similar steps of cellulosytic pathways, which benefited the system stability and activity (Wörner & Pester, 2019)	13.48%	–	10.70%
	<i>norank_o__SJA-28</i>	Heterotrophic bacteria benefited the reactor system stability and activity (avoiding from adverse environments), which can use lignocellulosic substrates (Su et al., 2022)	8.89%	9.69%	11.27%
	<i>norank_f__A4b</i>	Heterotrophic bacteria associated with the maintenance of system stability, which has the ability to degrade refractory organic matter (Jiang et al., 2023; Xu et al., 2022a)	5.46%	3.50%	3.46%
	<i>norank_f__Leptospiraceae</i>	<i>Leptospiraceae</i> sp. was associated with the secretion of lipopolysaccharides and can promote the formation of biofilms (Song et al., 2021)	3.04%	–	3.22%
	<i>norank_p__BRC1</i>	Heterotrophic bacteria may be linked to urease and/or catalase-producing, which has the potential to degrade refractory substances (Jokanović et al., 2021)	–	–	2.43%
	<i>norank_c__OM190</i>	Heterotrophic bacteria associated with cellulose decomposer (Chen et al., 2021)	–	–	1.89%
	HD	<i>norank_f__Anaerolineaceae</i>	<i>Anaerolineaceae</i> sp. played a crucial role in denitrification and benefitted the carbohydrate degradation for nitrogen removal by providing more readily available carbon source (Cao et al., 2020)	5.73%	–
	<i>norank_o__Chloroplast</i>	It means that the structure of the biofilm microbial community encouraged simultaneous nitrification and denitrification (Sun & Zheng, 2022; Zhang et al., 2018)	5.13%	6.84%	9.13%
	<i>norank_f__Caldilineaceae</i>	<i>Caldilineaceae</i> sp. closely associated with nitrogen removal (Cao et al., 2020; Fan et al., 2022)	4.05%	5.32%	–
	<i>norank_o__Ardenticatenales</i>	<i>Ardenticatena</i> sp. was identified denitrifying genera (Feng et al., 2020)	3.65%	8.77%	–
	<i>unclassified_f__Burkholderiaceae</i>	<i>Burkholderia</i> sp. was revealed as incomplete denitrifiers (Hetz & Horn, 2021)	–	2.96%	3.34%
	<i>Denitratisoma</i>	<i>Denitratisoma</i> sp. was highly related to heterotrophic denitrification (Chen et al., 2020)	–	2.14%	–
	<i>Limnobacter</i>	<i>Limnobacter</i> was heterotrophic sulfur oxidation and may adapt with anaerobic methane oxidizer bacteria (Algonin et al., 2023)	–	1.88%	–
	<i>Lentimicrobium</i>	The genus <i>Lentimicrobium</i> was known as a potential heterotrophic denitrifier (Dong et al., 2021; González-Cortés et al., 2023; Wang et al., 2021)	–	–	1.93%
AD	<i>Clostridium_sensu_stricto_12</i>	Previous literature showed that <i>Clostridium</i> was dominant species acted as key contributor to nitrate reduction in autotrophic denitrifying process (Xu et al., 2017)	–	4.41%	–
NFB	<i>Leptolyngbya_ANT.L52.2</i>	It may reduce nitrogen to usable ammonia (Lopardo et al., 2019)	3.48%	–	–

^a means relative abundances%; MOB means methane-oxidizing bacteria; HD means heterotrophic denitrifiers; PBB means promoting biofilm bacteria; NFB means nitrogen-fixing bacteria; AD means autotrophic denitrifiers; – means not in top 10

3.5 Implications from this work

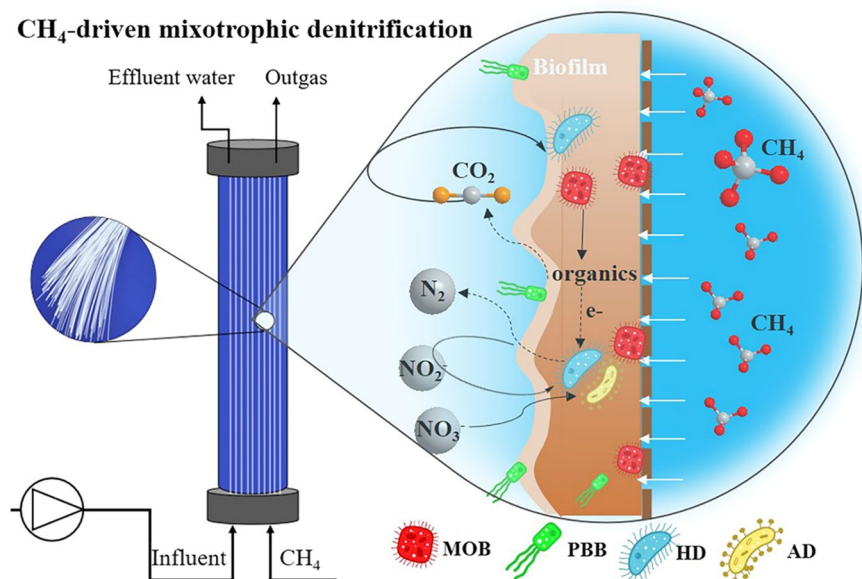
Wastewater is deemed as the fifth-largest source of global anthropogenic CH_4 emissions, approximately 7~9% in total. In fact, the removed COD and excess sludge yield was usually adopted as the activity data for estimating fugitive GHG emissions. It was reported that the China's national statistical emission of COD was 25.31 million tons in 2021, implying that considerable amount of CH_4 generated in China's municipal wastewater industry (Liu et al., 2015). For example, the emission factor values of CH_4 emissions produced vary strikingly among different conventional treatment processes during wastewater management, ranging from 0.05 to 12.90 g CH_4 /kg COD removal, while these values of wastewater sludge disposal (like landfill, land application, incineration, manufacturing, and dumping) were approximately 0.049–105.4 kg CH_4 /t dry matter of sludge (Du et al., 2023). To date, there are many attempts to explore the low-carbon wastewater treatment methods to reduce the carbon footprint of China's WWTPs. Introducing anaerobic methane oxidation coupled to denitrification as an alternative emerging treatment technology may allow more energy-efficient nitrogen removal, benefiting not only from saving in unit costs (energy and chemicals used) in the denitrification process, but also from the extra carbon credit achieved by using self-produced fugitive CH_4 . For example, in

comparison with other organic sources (the unit costs of methanol, acetic acid, and glucose are 2650, 3700, and 4000 ¥/t, respectively, while that of normalized electron donors required for each unit of NO_3^- -N removal are 1.068, 0.82, and 0.36, respectively), better unit-cost per electron donors (the product of the above two) may be achieved when using CH_4 as electron donor (Hao et al., 2023). However, lower denitrification rate ($0.42 \text{ mg/L}\cdot\text{h}^{-1}$) has been obtained in this work, suggesting that anaerobic methane oxidation coupled to other denitrification technologies might further improve the shortcomings of its strict demands of the work environment and growing slowly.

4 Conclusions

Reactivated stable CH_4 -driven denitrification processes were established in a MBfR. The biofilm system could be effectively recovered within 25 days after prolonged storage. With increasing influent NO_3^- -N concentration, the average denitrification rate of the reactor first increased and then decreased, also the microbial abundance in the reactor was improved. The highest average denitrification rate of $0.42 \text{ mg/L}\cdot\text{h}^{-1}$ was achieved at stage of influent NO_3^- -N of 20 mg/L, which was largest in diversity and lowest in evenness of microbial community. No

Fig. 6 Schematic diagram of synergetic system among promoting biofilm bacteria, methanotrophic bacteria, and denitrifiers for nitrate reducing



obvious NO_2^- -N and NH_4^+ -N accumulation in experiments. At the phylum level, the main phyla of microbial community in the reactor were *Proteobacteria*, *Chloroflexi*, and *Bacteroidetes*. At the class level, *Anaerolineae*, *Gammaproteobacteria*, *Ignavibacteria*, *Alphaproteobacteria*, *Oxyphotobacteria*, and *Chitinivibrionia* are the dominant classes. In addition, DAMO archaea and bacteria were not detected or were not dominant in the reactor. It speculated that the PBB became the key functional bacterial group after prolonged storage. Besides, MOB bacteria (e.g., *Methylocystis*), PBB, and denitrifiers jointly formed the system. This work may help understanding the applications of anaerobic CH_4 oxidation coupled to denitrification on low-carbon nitrogen removal.

Author Contribution Conceptualization: Hongyu Wang and Wei Zhang. Resources: Hongyu Wang. Methodology and data collection and analysis: Jing Wang and Wei Zhang. Funding acquisition: Wei Zhang and Shiquan Sun. Writing—original draft: Yibo Zhao. Writing—review and editing: Yang Gao, Lean Zhou, Shiquan Sun, Meiyi Tang, Yazhou Peng, and Wenbing Guo. All authors read and approved the final manuscript.

Funding This work was supported by the National Key Research and Development Program of China (2022YFE0105600) and the Natural Science Foundation of Hunan Province (2021JJ40606).

Data Availability All relevant data are included in the paper or its supplementary information.

Declarations

Conflict of Interest The authors declare no competing interests.

References

- Algonin, A., Zhao, B., Cui, Y., Xie, F., & Yue, X. (2023). Enhancement of iron-based nitrogen removal with an electric–magnetic field in an upflow microaerobic sludge reactor (UMSR). *Environmental Science and Pollution Research*, *30*, 35054–35063.
- Bhattacharjee, A. S., Motlagh, A. M., Jetten, M. S. M., & Goel, R. (2016). Methane dependent denitrification - From ecosystem to laboratory-scale enrichment for engineering applications. *Water Research*, *99*, 244–252.
- Cai, C. (2013). *Research on enrichment of denitrifying anaerobic methane oxidizing microorganisms*. Zhejiang University
- Cao, J., Zhang, T., Wu, Y., Sun, Y., Zhang, Y., Huang, B., Fu, B., Yang, E., Zhang, Q., & Luo, J. (2020). Correlations of nitrogen removal and core functional genera in full-scale wastewater treatment plants: Influences of different treatment processes and influent characteristics. *Bioresource Technology*, *297*, 122455.
- Cao, Q., Li, X., Jiang, H., Wu, H., Xie, Z., Zhang, X., Li, N., Huang, X., Li, Z., Liu, X. & Li, D. (2021). Ammonia removal through combined methane oxidation and nitrification-denitrification and the interactions among functional microorganisms. *Water Research*, *188*, 116555.
- Cao, X. K., Jiang, L., Zheng, H., Liao, Y., Zhang, Q., Shen, Q. S., Mao, Y. X., Ji, F. Y. & Shi, D. Z. (2022). Constructed wetlands for rural domestic wastewater treatment: A coupling of tidal strategy, in-situ bio-regeneration of zeolite and Fe (II)-oxygen denitrification. *Bioresource Technology*, *344*, 126185.
- Chen, D., Yang, K., & Wang, H. Y. (2016). Effects of important factors on hydrogen-based autotrophic denitrification in a bioreactor. *Desalination and Water Treatment*, *57*, 3482–3488.
- Chen, Y., Shao, Z., Kong, Z., Gu, L., Fang, J., & Chai, H. (2020). Study of pyrite based autotrophic denitrification system for low-carbon source stormwater treatment. *Journal of Water Process Engineering*, *37*, 101414.
- Chen, C., Gan, Z., Xu, R., & Meng, F. (2021). Cellulose-induced shifts in microbial communities and microbial interactions in an anoxic/aerobic membrane bioreactor. *Journal of Water Process Engineering*, *42*, 102106.
- Deiglmayr, K., Philippot, L., & Kandeler, E. (2006). Functional stability of the nitrate-reducing community in grassland soils towards high nitrate supply. *Soil Biology and Biochemistry*, *38*, 2980–2984.
- Ding, A., Zheng, P., Zhang, M., & Zhang, Q. (2017a). Impacts of electron donor and acceptor on the performance of electrorophic denitrification. *Environmental Science and Pollution Research*, *24*, 19693–19702.
- Ding, J., Lu, Y.-Z., Fu, L., Ding, Z.-W., Mu, Y., Cheng, S. H., & Zeng, R. J. (2017b). Decoupling of DAMO archaea from DAMO bacteria in a methane driven microbial fuel cell. *Water Research*, *110*, 112–119.
- Dong, K., Feng, X., Wang, W., Chen, Y., Hu, W., Li, H. & Wang, D. (2021). Simultaneous partial nitrification and denitrification maintained in membrane bioreactor for nitrogen removal and hydrogen autotrophic denitrification for further treatment. *Membranes*, *11*(12), 911.
- Du, W.-J., Lu, J.-Y., Hu, Y.-R., Xiao, J., Yang, C., Wu, J., Huang, B., Cui, S., Wang, Y., & Li, W.-W. (2023). Spatiotemporal pattern of greenhouse gas emissions in China's wastewater sector and pathways towards carbon neutrality. *Nature Water*, *1*, 166–175.
- Elmelouky, A., Mortadi, A., El, C. & Elmoznine, R. (2018). Impedance spectroscopy as a tool to monitor the adsorption and removal of nitrate ions from aqueous solution using zinc aluminum chloride anionic clay. *Heliyon*, *4*, e00536.
- Fan, X., Li, J., He, L., Wang, Y., Zhou, J., Zhou, J., & Liu, C. (2022). Co-occurrence of autotrophic and heterotrophic denitrification in electrolysis assisted constructed wetland packing with coconut fiber as solid carbon source. *Chemosphere*, *301*, 134762.
- Fazi, S., Amalfitano, S., Venturi, S., Pacini, N., Vazquez, E., Olaka, L. A., Tassi, F., Crognale, S., Herzsprung, P., Lechtenfeld, O. J., Cabassi, J., Capecciacci, F., Rossetti,

- S., Yakimov, M. M., Vaselli, O., Harper, D. M. & Butturini, A. (2021). High concentrations of dissolved biogenic methane associated with cyanobacterial blooms in East African lake surface water. *Communications Biology*, 4, 845.
- Feng, L., Yang, J., Yu, H., Lan, Z., Ye, X., Yang, G., Yang, Q., & Zhou, J. (2020). Response of denitrifying community, denitrification genes and antibiotic resistance genes to oxytetracycline stress in polycaprolactone supported solid-phase denitrification reactor. *Bioresource Technology*, 308, 123274.
- Ghafari, S., Hasan, M., & Aroua, M. K. (2008). Bio-electrochemical removal of nitrate from water and wastewater—A review. *Bioresource Technology*, 99, 3965–3974.
- González-Cortés, J. J., Quijano, G., Ramírez, M., & Cantero, D. (2023). Methane concentration and bacterial communities' dynamics during the anoxic desulfurization of landfill biogas under diverse nitrate sources and hydraulic residence times. *Journal of Environmental Chemical Engineering*, 11, 109285.
- Guo, X., Lai, C.-Y., Hartmann, E. M., & Zhao, H.-P. (2023). Heterotrophic denitrification: An overlooked factor that contributes to nitrogen removal in n-DAMO mixed culture. *Environmental Research*, 216, 114802.
- Hao, X. D., Sun, S. B., Li, J., & Wu, Y. Y. (2023). Research advances of methane oxidation coupled to nitrogen removal of wastewater. *Acta Scientiae Circumstantiae*, 43, 1–15.
- Harb, R., Lacin, D., Subasi, I. & Erguder, T. H. (2021a). Denitrifying anaerobic methane oxidation (DAMO) cultures: Factors affecting their enrichment, performance and integration with anammox bacteria. *Journal of Environmental Management*, 295, 113070.
- Harb, R., Laçin, D., Subaşı, I., & Erguder, T. H. (2021b). Denitrifying anaerobic methane oxidation (DAMO) cultures: Factors affecting their enrichment, performance and integration with anammox bacteria. *Journal of Environmental Management*, 295, 113070.
- Hetz, S. A. & Horn, M. A. (2021). Burkholderiaceae are key acetate assimilators during complete denitrification in acidic cryoturbated peat circles of the arctic tundra. *Frontiers in Microbiology*, 12, 628269.
- Jiang, M., Ji, S., Wu, R., Yang, H., Li, Y.-Y., & Liu, J. (2023). Exploiting refractory organic matter for advanced nitrogen removal from mature landfill leachate via anammox in an expanded granular sludge bed reactor. *Bioresource Technology*, 371, 128594.
- Jokanović, S., Kajan, K., Perović, S., Ivanić, M., Mačić, V., & Orlić, S. (2021). Anthropogenic influence on the environmental health along Montenegro coast based on the bacterial and chemical characterization. *Environmental Pollution*, 271, 116383.
- Khanina, L. G., Smirnov, V. E. & Bobrovskii, M. V. (2016). Species diversity of plant communities of Kaluga Zaseki Reserve: Estimation based on Shannon and Simpson indices and Hill's numbers. *Lesovedenie*, 1, 65–73.
- Lai, C.-Y., Lv, P.-L., Dong, Q.-Y., Yeo, S. L., Rittmann, B. E. & Zhao, H.-P. (2018). Bromate and nitrate bioreduction coupled with poly- β -hydroxybutyrate production in a methane-based membrane biofilm reactor. *Environmental Science & Technology*, 52, 7024–7031.
- Lee, D. J., Pan, X. L., Wang, A. J., & Ho, K. L. (2013). Facultative autotrophic denitrifiers in denitrifying sulfide removal granules. *Bioresource Technology*, 132, 356–360.
- Liang, L., Sun, C., Jin, Z., Wang, M., Yu, Q., Zhao, Z., & Zhang, Y. (2022). Magnetite-mediated electrically connected community for shortening startup of methane-dependent denitrification in a membrane biofilm reactor. *Chemical Engineering Journal*, 428, 132004.
- Liao, R. H., Li, Y., Yu, X. M., Shi, P., Wang, Z., Shen, K., Shi, Q. Q., Miao, Y., Li, W. T., & Li, A. M. (2014). Performance and microbial diversity of an expanded granular sludge bed reactor for high sulfate and nitrate waste brine treatment. *Journal of Environmental Sciences*, 26, 717–725.
- Lim, Z. K., Liu, T., Zheng, M., Yuan, Z., Guo, J., & Hu, S. (2021). Versatility of nitrite/nitrate-dependent anaerobic methane oxidation (n-DAMO): First demonstration with real wastewater. *Water Research*, 194, 116912.
- Liu, Y., Ni, B.-J., Sharma, K. R., & Yuan, Z. (2015). Methane emission from sewers. *Science of The Total Environment*, 524–525, 40–51.
- Liu, W.-H., Zhang, C.-G., Gao, P.-F., Song, Y.-Q., Huang, B.-S., & Yang, J.-F. (2019). Improved biological denitrification method for wastewater treatment. *Fresenius Environmental Bulletin*, 28, 6626–6631.
- Liu, S. F., Yu, X. L., Qin, H. M., Ye, J. S. & Long, Y. (2023). Newly isolated strain *methylocystis* sp. L03 oxidizes methane with nitrite as terminal electron acceptor. *Journal of Environmental Engineering*, 149, 04023084.
- Lopardo, C. R., Zhang, L., Mitsch, W. J., & Urakawa, H. (2019). Comparison of nutrient retention efficiency between vertical-flow and floating treatment wetland mesocosms with and without biodegradable plastic. *Ecological Engineering*, 131, 120–130.
- Lou, J. Q., Lv, J., & Yang, D. Y. (2020). Effects of environmental factors on nitrate-DAMO activity. *Water Air and Soil Pollution*, 231(6), 263.
- Lu, Y. Z., Chen, G. J., Bai, Y. N., Fu, L., Qin, L. P., & Zeng, R. J. X. (2018). Chromium isotope fractionation during Cr(VI) reduction in a methane-based hollow-fiber membrane biofilm reactor. *Water Research*, 130, 263–270.
- Luesken, F. A., Sanchez, J., van Alen, T. A., Sanabria, J., Op den Camp, H. J. M., Jetten, M. S. M., & Kartal, B. (2011). Simultaneous nitrite-dependent anaerobic methane and ammonium oxidation processes. *Applied and Environmental Microbiology*, 77, 6802–6807.
- Luo, J. H., Liang, H., Yan, L. J., Ma, J., Yang, Y. L., & Li, G. B. (2013). Microbial community structures in a closed raw water distribution system biofilm as revealed by 454-pyrosequencing analysis and the effect of microbial biofilm communities on raw water quality. *Bioresource Technology*, 148, 189–195.
- Massoudinejad, M., Ghaderpoori, M., Jafari, A., Nasehifar, J., Malekzadeh, A., & Ghaderpoury, A. (2018). Data on nitrate and nitrite of Taham dam in Zanjan (Iran). *Data in Brief*, 17, 431–437.

- Pang, Y. M., & Wang, J. L. (2020). Insight into the mechanism of chemoautotrophic denitrification using pyrite (FeS₂) as electron donor. *Bioresource Technology*, *318*, 124105.
- Pu, J. Y., Feng, C. P., Liu, Y., Li, R., Kong, Z., Chen, N., Tong, S., Hao, C. B., & Liu, Y. (2014). Pyrite-based autotrophic denitrification for remediation of nitrate contaminated groundwater. *Bioresource Technology*, *173*, 117–123.
- Puig, S., Coma, M., Desloover, J., Boon, N., Colprim, J., & Balaguer, M. D. (2012). Autotrophic denitrification in microbial fuel cells treating low ionic strength waters. *Environmental Science & Technology*, *46*, 2309–2315.
- Rahman, N. A., Parks, D. H., Vanwonterghem, I., Morrison, M., Tyson, G. W., & Hugenholtz, P. (2016). A phylogenomic analysis of the bacterial phylum fibrobacteres. *Frontiers in Microbiology*, *6*, 1469.
- Romanelli, A., Soto, D. X., Matiatos, I., Martinez, D. E., & Esquiú, S. (2020). A biological and nitrate isotopic assessment framework to understand eutrophication in aquatic ecosystems. *Science of the Total Environment*, *715*, 136909.
- Semrau, J. D., DiSpirito, A. A., & Vuilleumier, S. (2011). Facultative methanotrophy: False leads, true results, and suggestions for future research. *FEMS Microbiology Letters*, *323*, 1–12.
- Sepehri, A., & Sarrafzadeh, M. H. (2018). Effect of nitrifiers community on fouling mitigation and nitrification efficiency in a membrane bioreactor. *Chemical Engineering and Processing-Process Intensification*, *128*, 10–18.
- Sepehri, A., & Sarrafzadeh, M. H. (2019). Activity enhancement of ammonia-oxidizing bacteria and nitrite-oxidizing bacteria in activated sludge process: Metabolite reduction and CO₂ mitigation intensification process. *Applied Water Science*, *9*, 131.
- Shen, Y., Zhu, L., Ji, B., Fan, S. Q., Xiao, Y. B., & Ma, Y. Q. (2021). Reactivation of frozen stored microalgal-bacterial granular sludge under aeration and non-aeration conditions. *Water*, *13*, 1974.
- Shi, Y., Hu, S. H., Lou, J. Q., Lu, P. L., Keller, J., & Yuan, Z. G. (2013). Nitrogen removal from wastewater by coupling anammox and methane-dependent denitrification in a membrane biofilm reactor. *Environmental Science & Technology*, *47*, 11577–11583.
- Shu, D. T., He, Y. L., Yue, H., & Wang, Q. Y. (2015). Microbial structures and community functions of anaerobic sludge in six full-scale wastewater treatment plants as revealed by 454 high-throughput pyrosequencing. *Bioresource Technology*, *186*, 163–172.
- Smith, R. L., Howes, B. L., & Garabedian, S. P. (1991). In situ measurement of methane oxidation in groundwater by using natural-gradient tracer tests. *Applied and Environmental Microbiology*, *57*, 1997–2004.
- Song, Z., Su, X., Li, P., Sun, F., Dong, W., Zhao, Z., Wen, Z., & Liao, R. (2021). Facial fabricated biocompatible homogeneous biocarriers involving biochar to enhance denitrification performance in an anoxic moving bed biofilm reactor. *Bioresource Technology*, *341*, 125866.
- Su, B., Liu, Q., Liang, H., Zhou, X., Zhang, Y., Liu, G., & Qiao, Z. (2022). Simultaneous partial nitrification, anammox, and denitrification in an upflow microaerobic membrane bioreactor treating middle concentration of ammonia nitrogen wastewater with low COD/TN ratio. *Chemosphere*, *295*, 133832.
- Sun, W., & Zheng, Z. (2022). Research on removal of fluoroquinolones in rural domestic wastewater by vertical flow constructed wetlands under different hydraulic loads. *Chemosphere*, *303*, 135100.
- Vasiliadou, I. A., Karanasios, K. A., Pavlou, S., & Vayenas, D. V. (2009). Experimental and modelling study of drinking water hydrogenotrophic denitrification in packed-bed reactors. *Journal of Hazardous Materials*, *165*, 812–824.
- Wang, Y., Bott, C., & Nerenberg, R. (2016). Sulfur-based denitrification: Effect of biofilm development on denitrification fluxes. *Water Research*, *100*, 184–193.
- Wang, R., Yang, C., Zhang, M., Xu, S. Y., Dai, C. L., Liang, L. Y., Zhao, H. P., & Zheng, P. (2017). Chemoautotrophic denitrification based on ferrous iron oxidation: Reactor performance and sludge characteristics. *Chemical Engineering Journal*, *313*, 693–701.
- Wang, Z., He, S. B., Huang, J. C., Zhou, W. L., & Chen, W. N. (2018). Comparison of heterotrophic and autotrophic denitrification processes for nitrate removal from phosphorus-limited surface water. *Environmental Pollution*, *238*, 562–572.
- Wang, H., Sun, Y., Zhang, L., Wang, W., & Guan, Y. (2021). Enhanced nitrogen removal and mitigation of nitrous oxide emission potential in a lab-scale rain garden with internal water storage. *Journal of Water Process Engineering*, *42*, 102147.
- Wang, H., Qin, X. J., Mi, S., Li, X., Wang, X. L., Yan, W. J., & Zhang, C. H. (2019a). Contamination of yellow-feathered broiler carcasses: Microbial diversity and succession during processing. *Food Microbiology*, *83*, 18–26.
- Wang, H. Y., Lyu, W. L., Hu, X. L., Chen, L., He, Q. L., Zhang, W., Song, J. Y. & Wu, J. (2019b). Effects of current intensities on the performances and microbial communities in a combined bio-electrochemical and sulfur autotrophic denitrification (CBSAD) system. *Science of the Total Environment*, *694*, 133775.
- Wei, H. W., Wang, J., Hassan, M., Han, L., & Xie, B. (2017). Anaerobic ammonium oxidation-denitrification synergistic interaction of mature landfill leachate in aged refuse bioreactor: Variations and effects of microbial community structures. *Bioresource Technology*, *243*, 1149–1158.
- Wörner, S., & Pester, M. (2019). Microbial succession of anaerobic chitin degradation in freshwater sediments. *Applied and Environmental Microbiology*, *85*, e00963-e919.
- Xiao, Y., Zheng, Y., Wu, S., Yang, Z. H., & Zhao, F. (2015). Bacterial community structure of autotrophic denitrification biocathode by 454 pyrosequencing of the 16S rRNA gene. *Microbial Ecology*, *69*, 492–499.
- Xu, D., Xiao, E., Xu, P., Zhou, Y., He, F., Zhou, Q., Xu, D., & Wu, Z. (2017). Performance and microbial communities of completely autotrophic denitrification in a bioelectrochemically-assisted constructed wetland system for nitrate removal. *Bioresource Technology*, *228*, 39–46.
- Xu, J. J., Zhang, N., Xie, Z. Y., X. Y., Tang, L., Xia, J. F., & Yang, G. J. (2022a). Structural stability and microbial response mechanism of aerobic granular sludge exposed to perfluorooctane sulfonate. *China Environmental Science*, *42*, 5117–5127.

- Xu, P., Xie, Z., Shi, L., Yan, X., Fu, Z., Ma, J., Zhang, W., Wang, H., Xu, B., & He, Q. (2022b). Distinct responses of aerobic granular sludge sequencing batch reactors to nitrogen and phosphorus deficient conditions. *Science of the Total Environment*, 834, 155369.
- Zhang, M., Yang, Q., Zhang, J. H., Wang, C., Wang, S. Y., & Peng, Y. Z. (2016). Enhancement of denitrifying phosphorus removal and microbial community of long-term operation in an anaerobic anoxic oxic-biological contact oxidation system. *Journal of Bioscience and Bioengineering*, 122, 456–466.
- Zhang, R., Wang, L., Chen, P., & Pu, Y. (2018). Shifts in microbial community structure and diversity in a novel waterfall biofilm reactor combined with MBBR under light and dark conditions. *RSC Advances*, 8, 37462–37471.
- Zhou, J., Wang, H., Yang, K., Ji, B., Chen, D., Zhang, H., Sun, Y., & Tian, J. (2016). Autotrophic denitrification by nitrate-dependent Fe(II) oxidation in a continuous up-flow biofilter. *Bioprocess and Biosystems Engineering*, 39, 277–284.
- Zolnierczyk, M., & Barbusinski, K. (2019). Physicochemical methods of nitrate removal from wastewater. *Architecture Civil Engineering Environment*, 12, 153–159.

Publisher's Note Springer Nature remains neutral with regard to jurisdictional claims in published maps and institutional affiliations.

Springer Nature or its licensor (e.g. a society or other partner) holds exclusive rights to this article under a publishing agreement with the author(s) or other rightsholder(s); author self-archiving of the accepted manuscript version of this article is solely governed by the terms of such publishing agreement and applicable law.